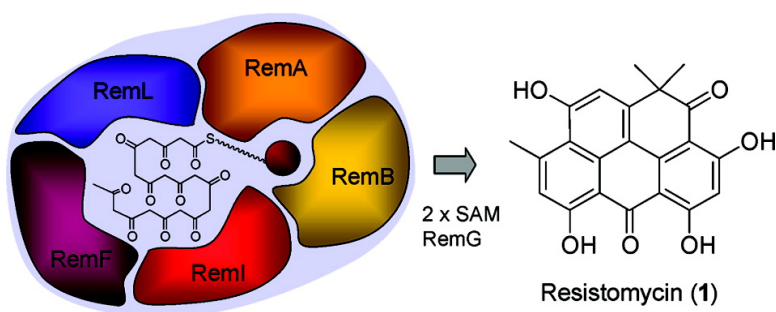


Orchestration of Discoid Polyketide Cyclization in the Resistomycin Pathway

Kathrin Fritzsche, Keishi Ishida, and Christian Hertweck

J. Am. Chem. Soc., **2008**, 130 (26), 8307-8316 • DOI: 10.1021/ja800251m • Publication Date (Web): 06 June 2008

Downloaded from <http://pubs.acs.org> on February 8, 2009



More About This Article

Additional resources and features associated with this article are available within the HTML version:

- Supporting Information
- Access to high resolution figures
- Links to articles and content related to this article
- Copyright permission to reproduce figures and/or text from this article

[View the Full Text HTML](#)

Orchestration of Discoid Polyketide Cyclization in the Resistomycin Pathway

Kathrin Fritzsche,[†] Keishi Ishida,[†] and Christian Hertweck^{*,†,‡}

Leibniz Institute for Natural Product Research and Infection Biology, HKI, Department of Biomolecular Chemistry, Beutenbergstr. 11a, 07745 Jena, Germany and the Friedrich-Schiller University, Jena, Germany

Received January 15, 2008; E-mail: christian.hertweck@hki-jena.de

Abstract: Resistomycin is a bacterial polyphenolic metabolite from *Streptomyces resistomycificus* with a unique pentacyclic “discoid” ring system that clearly differs from the typical linear or angular architectures of aromatic polyketides. The first comprehensive cyclase amino acid sequence–function correlation revealed that the enzymes directing the nascent polyketide chain into a peri-fused system clearly differ from canonical linear and angular cyclases. All genes that are required and sufficient for resistomycin (*rem*) biosynthesis were identified through systematic dissection and reconstitution of the type II polyketide synthase (PKS) complex. The minimal *rem* PKS and the first cyclase were successfully cross-complemented with orthologues from the linear tetracenomycin polyketide pathway, indicating that both dekaaketide pathways share early biosynthetic steps. In total three cyclases that are involved in discoid cyclization (*RemI*, *RemF*, and *RemL*) were identified by mutational analyses and in vivo pathway reconstitution. Analyses of the metabolic profiles of mutants expressing incomplete gene sets led to the discovery of a novel tetracenomycin derivative, *TcmR1*. The most surprising finding is that only the concerted action of the PKS and all three cyclases leads to the discoid ring structure. These results provide strong support for a model according to which the multienzyme complex forms a cage in which the polyketide is shaped, rather than a sequential cyclization of the polyketide chain by individual enzymes.

1. Introduction

Aromatic polyketides represent a diverse group of secondary metabolites with well-known representatives like the clinically relevant anthracyclines and tetracyclines.¹ In general, polycyclic phenolic compounds are assembled by type II polyketide synthases.^{1–3} A hallmark of these multienzyme complexes is the presence of a ketosynthase heterodimer (*KS α* and *KS β*) that catalyzes iterative Claisen condensations of thioesters with malonyl-CoA units. During this process a freestanding acyl carrier protein (ACP) serves as an anchor for the growing chain. Besides these minimal PKS components additional enzymes are required to direct the highly reactive poly- β -keto intermediates into particular reaction channels. In the presence of cyclases (CYC), cofactor-free enzymes that function “chaperone-like”, spontaneous aldol chemistry is efficiently suppressed.^{1,4} Typical primary products of type II PKS resulting from the concerted type II PKS action are polyphenols that can be classified as the linear tetracyclines, anthracyclines, benzoisochromanequinones, tetracenomycins, aureolic acids, and the angular angucyclines as well as a group of pentangular polyphenols. Numerous elaborate tailoring reactions are known that diversify the phenolic polycycles, such as oxygenation, alkylation, halogena-

tion, and glycosylation.⁵ Knowledge of these complex pathways has not only provided profoundly new insights into intriguing reaction cascades but also set the basis for rational engineering of novel drug candidates.^{5,6} However, considering the plethora of aromatic polyketide structures known it is quite remarkable all of the basic polyketide structures are formed by a U-shaped folding of the poly- β -keto intermediates. Consequently, only a limited number or modes of cyclizations is realized, and virtually all polyphenols have a linear or angular architecture.^{7,8}

A clear exception from this biosynthetic scheme is resistomycin (**1**),⁹ a polyphenol with multiple peri-fused rings. The rare naphthanthrene derivative was isolated by Brockmann and co-workers from a *Streptomyces resistomycificus* culture and was named after its remarkable inertness toward heat, acid, and base.¹⁰ Various biological assays revealed that resistomycin is active against Gram-positive bacteria and mycobacteria and that it inhibits HIV-1 protease as well as DNA and RNA polymerase.^{11–13} More recently, it has been shown that resistomycin also exerts

(5) Rix, U.; Fischer, C.; Remsing, L. L.; Rohr, J. *Nat. Prod. Rep.* **2002**, *19*, 542–580.

(6) Reeves, C. D. *Crit. Rev. Biotechnol.* **2003**, *23*, 95–147.

(7) Jakobi, K.; Hertweck, C. *J. Am. Chem. Soc.* **2004**, *126*, 2298–2299.

(8) Lackner, G.; Schenk, A.; Xu, Z.; Reinhardt, K.; Yunt, Z. S.; Piel, J.; Hertweck, C. *J. Am. Chem. Soc.* **2007**, *129*, 9306–9312.

(9) Brockmann, H.; Reschke, T. *Tetrahedron Lett.* **1968**, *27*, 3167–3170.

(10) Brockmann, H.; Schmidt-Kastner, G. *Naturwissenschaften* **1951**, *38*, 479–480.

(11) Haupt, I.; Eckardt, K. Z. *Allg. Mikrobiol.* **1972**, *12*, 573–579.

(12) Roggo, B. E.; Petersen, F.; Delmendo, R.; Jenny, H. B.; Peter, H. H.; Roedel, J. *J. Antibiot.* **1994**, *47*, 136–142.

(13) Bradler, G.; Eckardt, K. Z. *Allg. Mikrobiol.* **1972**, *12*, 535–545.

[†] Leibniz Institute for Natural Product Research and Infection Biology.

[‡] Friedrich-Schiller University.

(1) Hertweck, C.; Luzhetskyy, A.; Rebets, Y.; Bechthold, A. *Nat. Prod. Rep.* **2007**, *24*, 162–190.

(2) Rawlings, B. J. *Nat. Prod. Rep.* **1999**, *16*, 425–484.

(3) Shen, B. *Top. Curr. Chem.* **2000**, *209*, 1–51.

(4) Shen, Y.; Yoon, P.; Yu, T.-W.; Floss, H. G.; Hopwood, D.; Moore, B. S. *Proc. Natl. Acad. Sci. U.S.A.* **1999**, *96*, 3622–3627.

a modulating effect on apoptosis.¹⁴ The structure of resistomycin stands out because peri-fused carbocycles where the rings are fused through more than one face are extremely scarce among bacterial polyketide metabolites. Höfle and co-workers deduced from ¹³C isotope labeling studies that the unusual pentacyclic “discoïd” ring structure results from an unparalleled S-shaped folding and cyclization of a decaketide.^{15,16} Strikingly, a halogenated resistomycin derivative, chloroxanthomycin, has been isolated from a *Bacillus* species.¹⁷ Both the unusual folding pattern and the occurrence of related compounds in taxonomically distant bacterial species pointed toward an exceptional aromatic polyketide pathway. This was further corroborated by the finding that all attempts to identify the resistomycin (*rem*) gene locus by reverse genetics using known type II PKS sequences failed.⁷ Therefore we needed to employ a phenotype screening approach taking advantage of the intense orange fluorescence of **1**. By heterologous expression of a cosmid library pool we succeeded in cloning and sequencing the entire *rem* biosynthetic gene cluster, which set the foundation for studying the molecular basis of discoïd polyketide formation.⁷ Through mutational analyses we found that the geminal methyl groups are introduced by RemG,¹⁸ a novel type of bis-C-methyltransferase¹⁹ and that further hydroxylation by RemO²⁰ gives rise to the boat-shaped derivative resistoflavin.²¹

In the present study we provide the first comprehensive survey on polyketide cyclases and report on the functional characterization of all essential and sufficient components required for resistomycin biosynthesis. Furthermore, we demonstrate that only the concerted action of the noncanonical *rem* PKS or functionally equivalent decaketide synthases with a defined set of cyclases leads to discoïd polyketide formation.

2. Results and Discussion

2.1. A Phylogenetic Survey of Cyclases Involved in Bacterial Polyketide Biosynthesis.

The biosynthesis of the pentacyclic ring system of resistomycin requires the PKS and a set of cyclases to suppress spontaneous aldol condensations of the poly- β -keto intermediate. In silico analyses of the *rem* biosynthetic gene cluster yielded several additional candidates that could code for cyclases: *remL*, *remF*, and *remK*. However, the sequences of the deduced gene products show only low similarity/identity scores to known cyclases.⁷ We thus aimed at a more extensive sequence analysis to compare cyclases and to assign their tentative functions. Surprisingly, no comprehensive phylogenetic survey on cyclases has yet been reported. Being aware that such an analysis is formally critical because

of the versatility of this family of proteins, we assumed that a phylogenetic survey based on the amino acid sequences would aid identifying types of cyclases that are involved in similar cyclization processes. Approximately 100 putative and verified cyclase amino acid sequences were retrieved through database searches and aligned with ClustalX. By means of the robust neighbor joining (NJ) algorithm and bootstrapping a well-supported phylogenetic tree was obtained (Figure S1). The color-coded cladogram (Figure 1) shows that, at least in principle, the ring topology correlates well with the types of cyclases. In regard to first and second cyclizations it should be noted that many studies on minimal PKS revealed that the first ring cyclization is mainly controlled by the minimal PKS. Nonetheless, the cyclization of the first two rings is supported by cyclases and aromatases, and it is possible that cyclases stabilize the PKS thus preventing aberrant first cyclization. Such typical (first and) second ring cyclases can be found in clades VII, VIII, IX, and X. Clades VIII and IX comprise enzymes with dual first ring cyclase-aromatase functions in linear polyphenol pathways (i.e., clade VIII, aureolic acids and benzoisochromanequinones; clade IX, anthracyclines and tetracyclines). The related clade X contains first ring cyclases from angucyclic pathways. Phylogenetically more distant is clade VII with various orthologues from linear (e.g., elloramycin) and pentangular (e.g., benastatin) pathways. The sequence of the well characterized first and potentially second ring cyclase TcmN^{22–24} clusters with this group, and RemI seems to represent a related cyclase. Second and third ring cyclases involved in the linear anthracycline, tetracycline, and aureolic acid pathways can be found in clade II. These enzymes seem to be weakly related to the putative cyclase RemL, which shares the conserved HxGTHxDxPxH motif. It seems that pigments as well as linear tetracyclic and pentangular polyketide pathways share similar types of proteins, and also the putative cyclase RemF could be assigned to clade I. Notably, all proteins in this group share a cupin motif.²⁵ The final cyclizations in the various polyketide pathways are catalyzed by members of clades III–VI. Pyran formation of BIQs is catalyzed by enzymes that are similar to Zn-dependent hydrolases (metallo beta lactamase family, clade III). Other linear polyketide pathways (tetracycline, aureolic acids, and anthracyclines) involve third and fourth ring cyclases from clades VIa, which is represented by the tetrameric SnaoL²⁶ and a rather inhomogenous clade VIb. Within this group, the function of StfX as a fourth ring cyclase has been experimentally proven,²⁷ while OxyI does not seem essential for complete assembly of the amidated tetracyclic aglycone.²⁸ Angular systems seem to employ quite distinct cyclases that form clades IV (3rd/4th ring cyclases that occur as cyclase/dehydrase didomain enzymes in angucycline pathways) and clade V (putative 4th/5th ring cyclases in pentangular pathways),

(14) Shiono, Y.; Shiono, N.; Seo, S.; Oka, S.; Yamazaki, Y. *Z. Naturforsch.* **2002**, *57c*, 923–929.

(15) Höfle, G.; Wolf, H. *Liebigs Ann. Chem.* **1983**, 835–843.

(16) (a) A very similar folding is only observed for fungal phenalenone metabolites: Simpson, T. J. *J. Chem. Soc., Perkin Trans. 1*, **1979**, 1, 1233–1238. (b) Hata, K.; Baba, K.; Kozawa, M. *Chem. Pharm. Bull.* **1978**, *26*, 3792–3797. (c) Diaz, F.; Chai, H.-B.; Mi, Q.; Su, B.-N.; Vigo, J. S.; Graham, J. G.; Cabieses, F.; Farnsworth, N. R.; Cordell, G. A.; Pezzuto, J. M.; Swanson, S. M.; Kinghorn, A. D. *J. Nat. Prod.* **2004**, *67*, 352–356.

(17) Magyarosy, A.; Ho, J. Z.; Rapoport, H.; Dawson, S.; Hancock, J.; Keasling, J. D. *Appl. Environ. Microbiol.* **2002**, *68*, 4095–4101.

(18) Ishida, K.; Fritzsche, K.; Hertweck, C. *J. Am. Chem. Soc.* **2007**, *129*, 12648–12649.

(19) Schenk, A.; Xu, Z.; Pfeiffer, C.; Steinbeck, C.; Hertweck, C. *Angew. Chem., Int. Ed.* **2007**, *46*, 7035–7038.

(20) Ishida, K.; Maksimenka, K.; Fritzsche, K.; Scherlach, K.; Bringmann, G.; Hertweck, C. *J. Am. Chem. Soc.* **2006**, *128*, 14619–14624.

(21) Eckardt, K.; Bradler, G.; Tresselt, D.; Fritzsche, H. *Adv. Antimicrob. Antineoplast. Chemother.* **1972**, *1*, 1025–1027.

(22) Shen, B.; Hutchinson, C. R. *Proc. Natl. Acad. Sci. U.S.A.* **1996**, *93*, 6600–6604.

(23) Shen, B.; Summers, R. G.; Wendt-Pienkowski, E.; Hutchinson, C. R. *J. Am. Chem. Soc.* **1995**, *117*, 6811–6821.

(24) McDaniel, R.; Hutchinson, C. R.; Khosla, C. *J. Am. Chem. Soc.* **1995**, *117*, 6805–6810.

(25) Chin, K. H.; Chou, C. C.; Wang, A. H.; Chou, S. H. *Proteins* **2006**, *65*, 1046–1050.

(26) Sultana, A.; Kallio, P.; Jansson, A.; Wang, J. S.; Niemi, J.; Mantsala, P.; Schneider, G. *EMBO J.* **2004**, *23*, 1911–1921.

(27) Gullón, S.; Olano, C.; Abdelfattah, M. S.; Braña, A. F.; Rohr, J.; Méndez, C.; Salas, J. A. *Appl. Environ. Microbiol.* **2006**, *72*, 4172–4183.

(28) Zhang, W.; Watanabe, K.; Wang, C. C.; Tang, Y. *J. Biol. Chem.* **2007**, *282*, 25717–25725.

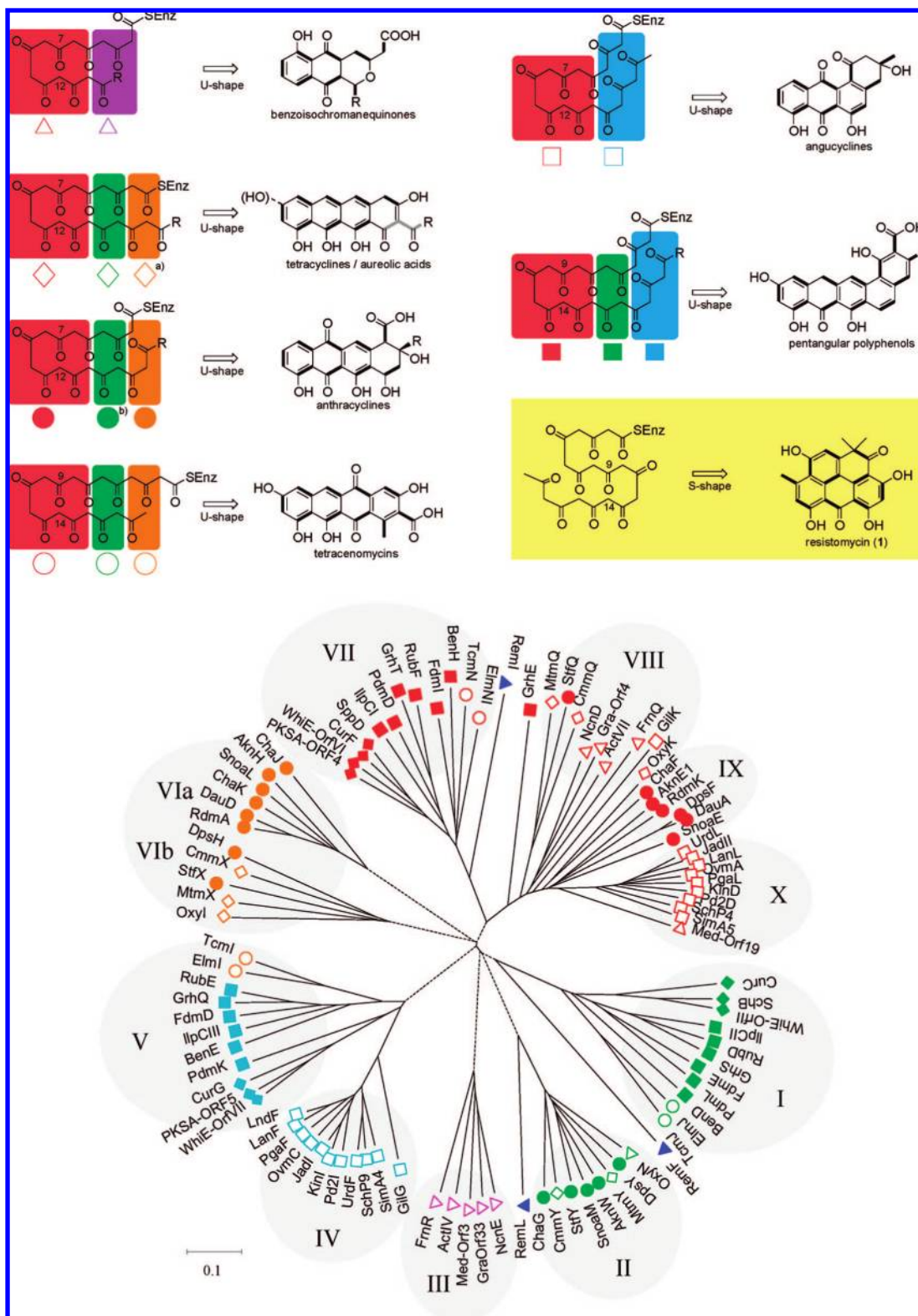


Figure 1. Cyclization pattern and ring topologies in aromatic polyketides produced by type II PKS. The color code refers to the function of the cyclases and the type of pathway involved. triangle, BIQs; filled triangle, discoid; circle, tetracenomycins; filled circle, anthracyclines; diamond, aureolic acids and tetracyclines; filled diamond, pigments; square, angucyclines; filled square, pentangular polyphenols. Acetate building blocks are highlighted in bold. ^aNot essential in oxytetracycline pathway; ^bmay also act as 2nd/3rd ring cyclase (top). Cladogram (NJ tree) showing clusters of related cyclases. Different groups of enzymes are separated by dotted connecting lines (bottom).

respectively. A surprising observation is that cyclases from linear tetracenomycin pathways (TcmI and ElmI) cluster with cyclases from pentangular systems, a similar scenario as in clades I and VII.

Taken together, the sequences of the cyclases correspond well with their proposed functions in virtually all type II PKS machineries and might be used as a roadmap to predict a polyphenolic pathway based on the deduced cyclase sequence.

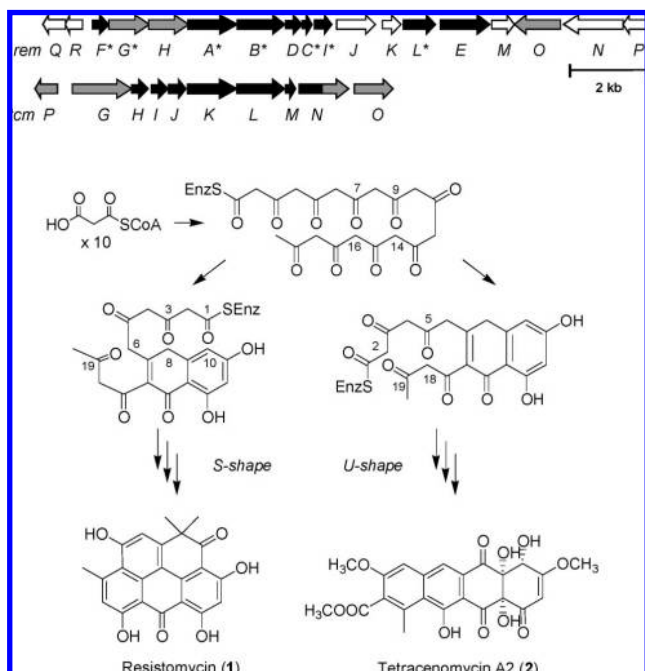


Figure 2. Architecture of the *rem* and *tcm* biosynthesis gene clusters. Black ORFs: PKS, cyclase, and other accessory genes. Gray ORFs: genes coding for tailoring enzymes. White ORFs: genes of unknown function; genes essential for *rem* biosynthesis are marked with an asterisk (*). Structures of the decaketides resistomycin and tetracenomycin resulting from discoid (S-shape) and linear (U-shape) cyclization, respectively.

However, the cladogram also shows its limitations in the case of the putative resistomycin cyclases. It is obvious that the cyclases involved in the biosynthesis of a discoid polyketide do not fit into the conventional scheme.

2.2. The linear tetracenomycin and discoid resistomycin pathways share early biosynthetic steps. The finding that putative cyclases involved in the resistomycin pathway are distinct from cyclases that shape linear and angular polyphenols is in line with the noncanonical nature of the resistomycin minimal PKS. Analysis of the gene locus encoding resistomycin biosynthesis suggested that open reading frames (ORFs) *rem-ABC* code for the minimal PKS required for polyketide assembly. Independent phylogenetic analyses by Bode et al. and our group revealed that the *rem* ketosynthase heterodimer RemAB is distant from the classical type II PKS enzymes known from actinomycetes and more similar to the yet only known type II PKS from the Gram-negative bacteria *Stigmatella aurantiaca*²⁹ and *Photorhabdus luminescens*.³⁰ The designated *rem* acyl carrier protein (RemC) is strikingly similar to fatty acid synthase ACPs. The apoenzyme is likely transformed into the holo-ACP by the gene product of *remD*, a putative phosphopantetheinyl transferase (PPTase). RemE, a protein with a similarity to AT domains from modular type I PKS, is not required for polyketide biosynthesis (K.F. and C.H., unpublished observations).

Irrespective of the noncanonical nature of the minimal *rem* PKS we assumed that resistomycin shares early biosynthetic steps with the linear decaketide tetracenomycin and that the first ring closure should be identical (Figure 2). Hutchinson and co-

workers have shown that expression of the minimal tetracenomycin (*tcm*) PKS with or without the first and second ring cyclase TcmN' (the N-terminus of the multifunctional cyclase-dehydratase-methyltransferase TcmN) yields two main products.^{22,31,32} In the absence of TcmN' the decaketide chain is folded at C-9, inducing a C-7/12 cyclization. Subsequent spontaneous cyclizations yield **SEK15**.³³ In the presence of TcmN' the first cyclization occurs between C-9 and C-14, yielding **RM80** as well as the dehydration product **RM80b**.²⁴ The high sequence similarity of RemI with TcmN' suggested that the nascent poly- β -keto intermediate is folded and cyclized in analogy to tetracenomycin biosynthesis. To validate this assumption we first constructed a gene cassette coding for the minimal PKS and the first ring cyclase, *remABDCI* (Figure S4). This cassette was cloned into expression vector pKJ55^{8,34} downstream of the constitutive *ermE* promoter and then introduced into *S. lividans* TK23. The broth of the transformant (*S. lividans* TK23/pKJ108) was screened for the expected shunt products. However, despite many attempts expression of *remABDCI* did not result in the production of detectable amounts of polyketides. By MS analysis only traces of compounds with M:384 could be identified, which might indicate the formation of metabolites such as **SEK15** or **RM80**. To rule out any mutations we complemented the lacking pathway genes. For this purpose, the *remABDCI* gene cassette was excised from cosmid pKJ05 by PCR-targeted recombination using primers KJrem09 and KJrem10. Through coexpression of the resulting plasmid (pKJ81, Δ *remABDCI*, *tsr*^R) and pKJ108 in *S. lividans* TK23 we succeeded in restoring resistomycin biosynthesis, as shown by HPLC-MS analysis. This result proves that a functional set of proteins, RemABDCI, was indeed produced and suggests that the performance of the *rem* PKS is context-dependent. Apparently, the PKS only functions properly or is sufficiently stabilized in the presence of additional pathway enzymes. In the case of enterocin biosynthesis, it has been shown that the minimal PKS does not yield polyketides unless a functional ketoreductase is coexpressed.^{35,36}

To demonstrate the functional identity of the initial pathway enzymes of the *tcm* and *rem* we then sought to complement the Δ *remABDCI* mutant with corresponding *tcm* biosynthetic genes. Plasmid pWHM732, a derivative of pWHM4*, which harbors a *tcmJKLMN* cassette,²² appeared to be suitable. It contains the minimal PKS genes (*tcmKLM*) as well as a gene coding for the first cyclase, TcmN', and TcmJ, which is known to increase polyketide yields.^{31,37} In order to achieve the coexpression of the incomplete *rem* gene set with the *tcm* genes, the *tsr*^R resistance cassette in pKJ81 needed to be exchanged for *aac(3)IV* by recombination in *E. coli*. The resulting plasmid, pKJ87, was introduced together with pWHM732 (*tcmJKLMN*', *tsr*^R) into *S. lividans* TK23 by protoplast transformation. While the negative control (*S. lividans* TK23/pKJ87+pWHM4*) did

(31) Bao, W.; Wendt-Pienkowski, E.; Hutchinson, C. R. *Biochemistry* **1998**, *37*, 8132–8138.

(32) Summers, R. G.; Wendt-Pienkowski, E.; Motamedi, H.; Hutchinson, C. R. *J. Bacteriol.* **1992**, *174*, 1810–1820.

(33) Fu, H.; Ebert-Khosla, S.; Hopwood, D. A.; Khosla, C. *J. Am. Chem. Soc.* **1994**, *116*, 4166–4170.

(34) Xu, Z.; Schenk, A.; Hertweck, C. *J. Am. Chem. Soc.* **2007**, *129*, 6022–6030.

(35) Piel, J.; Hertweck, C.; Shipley, P.; Hunt, D. S.; Newman, M. S.; Moore, B. S. *Chem. Biol.* **2000**, *7*, 943–955.

(36) Hertweck, C.; Xiang, L.; Kalaitzis, J. A.; Cheng, Q.; Palzer, M.; Moore, B. S. *Chem. Biol.* **2004**, *11*, 461–468.

(37) Summers, R. G.; Wendt-Pienkowski, E.; Motamedi, H.; Hutchinson, C. R. *J. Bacteriol.* **1993**, *1993*, 7571–7580.

(29) Sandmann, A.; Dikschat, J.; Jenke-Kodama, H.; Kunze, B.; Dittmann, E.; Müller, R. *Angew. Chem., Int. Ed.* **2007**, *46*, 2712–2716.

(30) Brachmann, A. O.; Joyce, S. A.; Jenke-Kodama, H.; Schwär, G.; Clarke, D. J.; Bode, H. B. *ChemBioChem* **2007**, *8*, 1721–1728.

not show any sign of polyketide production, the second control strain, *S. lividans* TK23/pWHM732, produced the typical *tcm* shunt products. In contrast, the strain expressing *rem* and *tcm* pathway genes proved to be capable of resistomycin production (Figure S2). The successful reconstitution of resistomycin biosynthesis suggested that TcmKLMN and RemABCI are functionally equivalent and that the initial steps in resistomycin and tetracenomycin are in fact congruent. Our next goal was to search for additional components of the biosynthetic pathway that lead to the divergence of the linear and discoid pathways.

2.3. Identification of Cyclases Sufficient and Essential for Discoid Polyketide Cyclization and Characterization of Shunt Products. Analyses of the *rem* biosynthetic gene cluster yielded several additional candidates that could code for cyclases. According to phylogeny and complementation experiments RemI would act as a first and second ring cyclase like TcmN'. In addition to the above-mentioned putative cyclases RemL and RemF, we also considered RemK, which did not show any similarity to known type II PKS components. To determine the function of these enzymes and the order of the cyclization steps all putative cyclase genes were individually deleted in the *rem* gene cluster. We succeeded in the inactivation of all genes except for *remI*, the function of which was deduced from cross-complementation. All mutated gene clusters were then introduced into *S. lividans* TK23 for expression, and the metabolic profiles were analyzed by HPLC-MS.

Deletion of *remK* in the *rem* gene cluster did not affect resistomycin biosynthesis; the polyketide was still produced by the $\Delta remK$ mutant at wild type titers. Consequently, RemK does not play any significant role in resistomycin biosynthesis. In contrast, the $\Delta remL$ mutant proved to be incapable of resistomycin production. Instead, at least one new compound with M: 384 was detected in the extract. To exclude polar effects, *remL* was PCR-amplified, sequenced, and ligated into the *Bam*HI/*Eco*RI sites of pKJ55, yielding pKJ105. Coexpression of the genes on plasmids pKJ75 and pKJ105 in *S. lividans* TK23 successfully restored resistomycin production. To characterize the polyketide metabolites formed by the $\Delta remL$ mutant, *S. lividans* TK23/pKJ75 was cultured on R5 agar. Open column chromatography and preparative RP-HPLC afforded the known decaketides **RM80b**, the dehydration product of **RM80**, and **SEK15**^{24,38} in a ratio of 10:1 (Figure 3).

Next, the putative cyclase gene *remF* was inactivated by in frame deletion. After FLP-mediated excision of the resistance cassette an 81 bp scar sequence containing a stop codon was introduced, resulting in a significantly truncated 297 bp ORF on plasmid pKJ123. HPLC analysis clearly indicated that the *S. lividans* TK23 transformant harboring plasmid pKJ123 did not produce resistomycin. Genetic complementation was achieved by coexpression of native *remF* on the pKJ55 derivative p128 in analogy to the above-mentioned protocol. In the mutant's culture broth several polyketide metabolites were detected. The known tetracenomycins **TcmD3** and **TcmD1** could be identified by comparison of HPLC retention times, UV spectra, and MS data with authentic references (Figure 4). Furthermore, two new compounds were detected that appeared to be related metabolites with similar UV spectra. Their molecular masses (M: 380 and M: 336, respectively) suggested that they differ in the loss of a carboxy group. To elucidate the structures of the main product *S. lividans* TK23/pKJ123 was grown on R5 plates and the extract was subjected to open column chromatography and

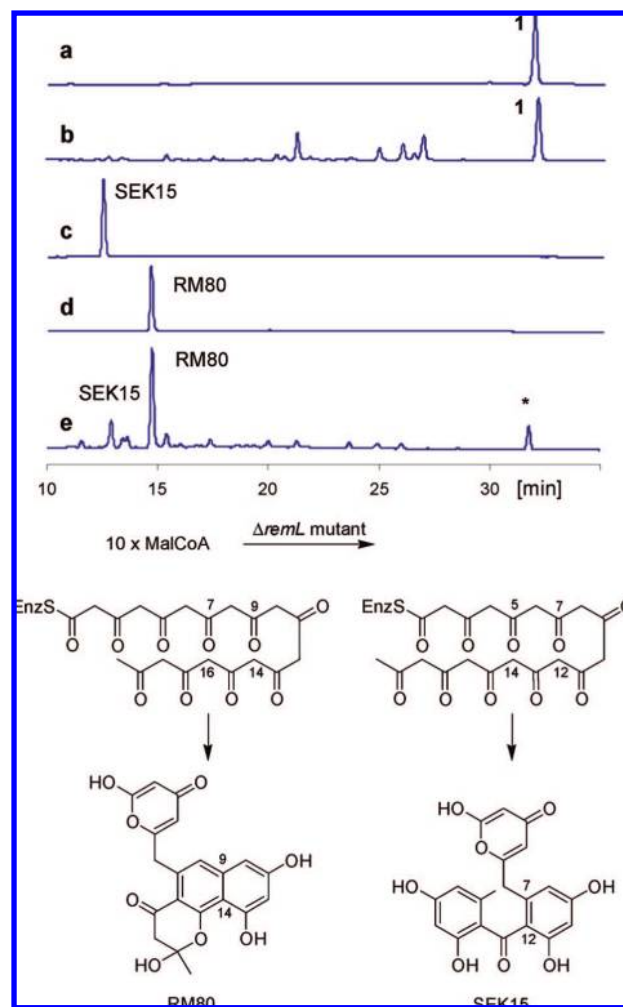


Figure 3. Results from mutational analyses. HPLC profiles of (a) resistomycin reference, (b) extract from wild type producer, (c) SEK15 reference, (d) RM80 reference, (e) mutant lacking *remL* (the marked * peak does not relate to resistomycin according to UV and MS data). Below: model for the formation of shunt metabolites through regiodivergent cyclization.

preparative RP-HPLC. Negative ion ESI-MS m/z 379 $[M - H]^-$ of the new compound was identical to that of **TcmD3**. However, while **TcmD3** is orange, the new compound was obtained as a dark purple solid. Also its 1H and ^{13}C NMR data were similar to those of **TcmD3**. In the 1H NMR spectrum, four singlet aromatic protons (δ 7.87, 7.64, 6.92, 6.57) and one aromatic methyl proton (δ 2.73) were detected. The ^{13}C NMR spectrum indicated two keto groups, several aromatic carbons bearing oxygen, and primarily aromatic carbons. The HMBC and HMQC spectra revealed that the structure of the new metabolite, named tetracenomycin R1 (**TcmR1**), differs from **TcmD3** in the position of the quinone moiety. The chemical analysis was impaired because a carbon signal at position either 1 or 15 was not detected or overlapped with another carbon in the ^{13}C NMR spectrum. Therefore tetracenomycin R1 methyl ester was prepared using trimethylsilyldiazomethane. NMR data of the derivative unequivocally allowed an assignment of carbon signal δ 158.5 to position 15. However, the HMBC correlations suggested two possible structures which might be formed tautomers at position 15 and 17. A comparison of NMR data with predicted ^{13}C chemical shifts (using ACD/Laboratories ver. 8.09, Advanced Chemistry Development Inc., Canada) indicated that the proposed structure of **TcmR1** represents the more stable

(38) Fu, H.; Hopwood, D. A.; Khosla, C. *Chem. Biol.* **1994**, *1*, 205–210.

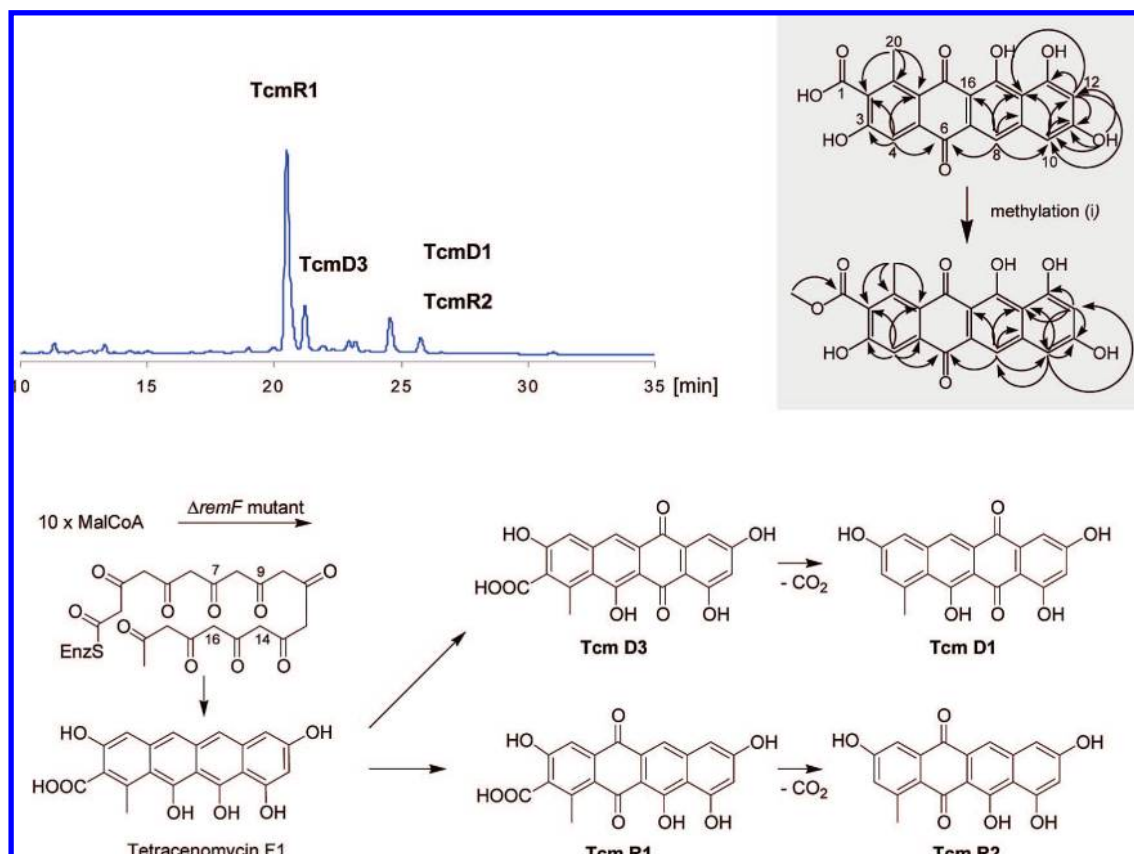


Figure 4. Results from mutational analyses. HPLC profile of extract from mutant lacking *remF*. Structure of tetragenomycin R and its methyl ester obtained by methylation and relevant C–H correlations. The shown tautomer is most likely according to calculated chemical shifts and spectra simulation; (i) trimethylsilyldiazomethane, methanol/benzene, rt. Model for the formation of tetragenomycins.

form and that the shown tautomer corresponds well with calculated chemical shifts. **TcmR1** obviously results from a regiodivergent oxygenation of the primary polyketide product, either spontaneously or catalyzed by a yet unknown anthrone oxidase. The amount of the minor product (**TcmR2**) with M: 336 was too small for a full structure elucidation, but MS data and UV suggested that the metabolite results from decarboxylation of **TcmR1** (Figure 4).

Summing up, the inactivation and complementation experiments clearly indicate that the cyclases *RemF* and *RemL* are crucial for discoid polyketide biosynthesis. We next needed to identify the set of enzymes that is sufficient for resistomycin biosynthesis.

2.4. Reconstitution of the Minimal Set of Genes Required for Discoid Polyketide Biosynthesis. Mutational studies indicated that several genes of the *rem* gene cluster are not essential for resistomycin biosynthesis. As shown above, expression of *remK*, *remH*, *remE*, and *remM*, *remN*, and *remP* is not required for polyketide formation. Furthermore, on the basis of homology searches it appeared unlikely that *remQRJ* were involved in the biosynthetic pathway. The minimal set of *rem* genes that codes for all necessary pathway enzymes and proteins should be represented by the minimal PKS genes, *remABC*, the parent PPTase gene (*remD*), the cyclase genes *remFIL*, and the bis-*C*-methyltransferase gene *remG*. To test this hypothesis, *rem* biosynthesis was restored in the heterologous host. Genes coding for the minimal PKS, *RemABDC*, and the first ring cyclase, *RemI*, were successively complemented with *remFGL* using a second, compatible vector (Table 1, Figures S3, S5).

Table 1. Survey on Gene Inactivation and Coexpression Experiments^a

| plasmid 1 | plasmid 2 | polyketide metabolites |
|----------------------------------|------------------------------|--|
| pKJ05 (<i>rem</i> gene cluster) | - | resistomycin |
| pKJ81 ($\Delta remABDCI$) | - | n.d. |
| pKJ81 ($\Delta remABDCI$) | pKJ108 (<i>remABDCI</i>) | resistomycin |
| pKJ87 ($\Delta remABDCI$) | pWHM732 (<i>tcmJKLMN'</i>) | resistomycin, <i>tcm</i> shunt metabolites |
| pKJ79 ($\Delta remK$) | - | resistomycin |
| pKJ123 ($\Delta remF$) | - | TcmR1, TcmR2, TcmD3, TcmD1 |
| pKJ123 ($\Delta remF$) | pKJ124 (<i>remF</i>) | resistomycin* |
| pKJ75 ($\Delta remL$) | - | RM80 and SEK15 |
| pKJ75 ($\Delta remL$) | pKJ105 (<i>remL</i>) | resistomycin* |
| pKJ108 (<i>remABDCI</i>) | - | n.d. |
| pKJ108 (<i>remABDCI</i>) | pKJ104 (<i>remL</i>) | TcmD3, TcmD1 |
| pKJ108 (<i>remABDCI</i>) | pKJ134 (<i>remGL</i>) | TcmD3, TcmD1 |
| pKJ108 (<i>remABDCI</i>) | pKJ133 (<i>remFGL</i>) | resistomycin* |

^a *, with background of shunt metabolites; n.d., none detected.

Expression of gene sets lacking *remF* (*remABDCIL* or *remABDCIGL*) does not lead to resistomycin production. Instead, TcmD3 and the decarboxylation product TcmD1 are formed. Only after addition of the cyclase gene *remF* was resistomycin biosynthesis observed. Thus, the *remABDCIFGL* cassette is required and sufficient for all resistomycin biosynthetic steps. The occurrence of TcmD3 and TcmD1 in the extract of *S. lividans* TK23/pKJ108+pKJ133 can be explained by the different titers of enzymes produced by the two-plasmid system.

As we have shown earlier the geminal bis-methylation represents the last step in resistomycin biosynthesis and does

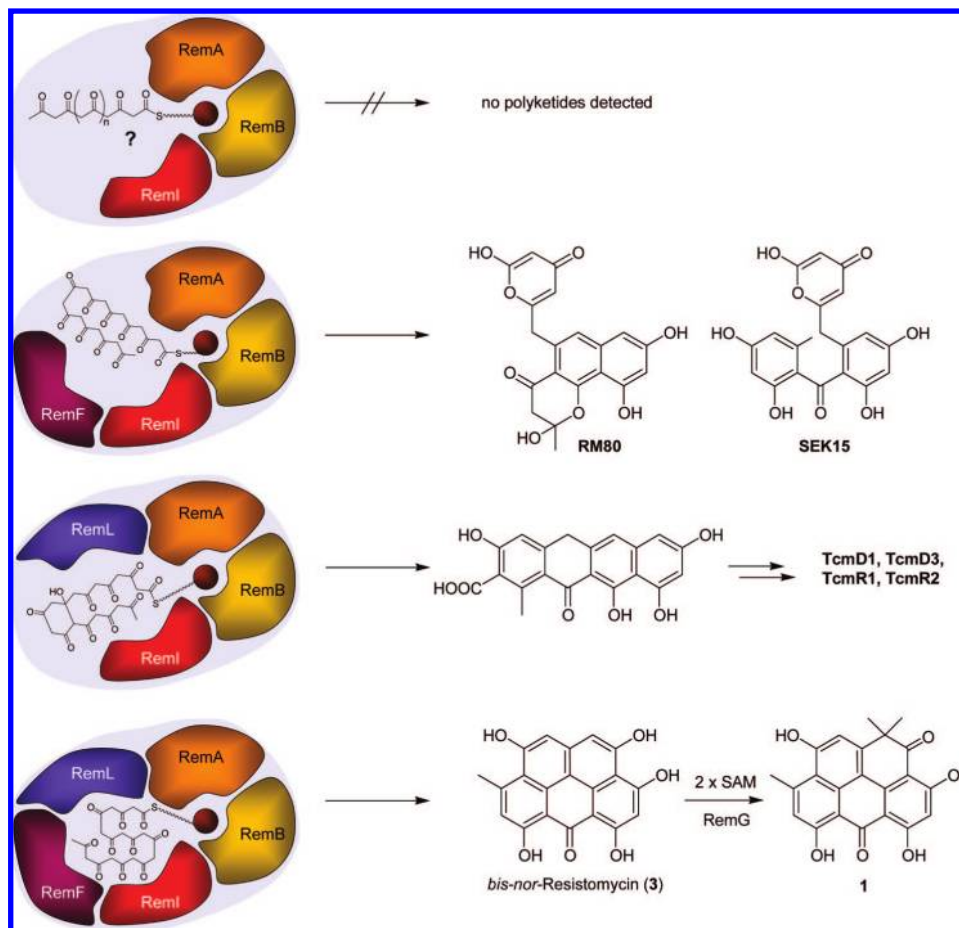


Figure 5. Model for controlled cyclization in a cage-like multienzyme complex, yielding a discoid polyketide only when type II PKS complex is intact.

not contribute to discoid cyclization. This is supported by the observation that the shunt products are not methylated. Furthermore, in the absence of the unusual bis-*C*-methyltransferase RemG, bis-norresistomycin (**3**) is produced.

2.5. Discoid polyketide formation requires the concerted action of all PKS and cyclase components. Cyclases are considered the key to diverse aromatic polyketide ring topologies. Although a high number of putative cyclases have been identified through molecular studies, only a few enzymes have been biochemically characterized (ester cyclase SnoaL,²⁶ cyclases ElmI,³⁹ DnrD,⁴⁰ TcmI,⁴¹ TcmN',²² and AknH⁴²), and the knowledge on the exact mechanisms of shaping and folding the nascent polyketide chains is still limited. In general, functional analyses of these enzymes are confined because of the inherent instability of the polyketide intermediates. From gene swapping and mutational studies and elucidation of the shunt metabolites or pathway intermediates produced it was concluded that cyclases could be attributed to individual cyclization steps, such as second ring, third ring, and so forth.^{1–3} This dissection strategy has proven feasible in angular and linear pathways leading to angucyclines,^{43,44} anthracyclines,^{27,45,46} tetracenomycins,^{22,37} and tetracyclines,^{28,47} respectively.

Our heterologous expression experiments now demonstrate that the cyclases RemI, RemF, and RemL are essential and sufficient to direct the S-shape folding of the decaketide produced by RemABCD. Because of the functional identity of RemABCI with TcmKLMN' we initially concluded that RemF and RemL are specialized in the discoid cyclization. Nonetheless, in the absence of either RemF or RemL, only linear tetracenomycin-like shunt products or randomly cyclized polyketides are produced. These results provide strong evidence that, at least in the resistomycin pathway, a defined complex of PKS and cyclases is needed to establish a cage-like cavity in which the growing polyketide chain is folded. It appears that only the intact multienzyme complex yields the discoid ring system (Figure 5). If one cyclase is missing, the protein association is impaired and shunt products result from spontaneous cyclizations of the highly reactive poly- β -keto intermediates. This model is supported by the surprising observation that RemABDCI alone does not lead to a detectable amount of polyketides. At least one additional cyclase is needed for efficient polyketide formation and/or release of the polyketide intermediate. Thus, this system represents a new example of a synergism of PKS with accessory enzymes, although mechanistically it clearly deviates from earlier observations of context-dependent type II PKS.^{36,48}

(39) Rafanan, E. R., Jr.; Le, L.; Zhao, L.; Decker, H.; Shen, B. *J. Nat. Prod.* **2001**, *64*, 444–449.

(40) Kendrew, S. G.; Katayama, K.; Deutsch, E.; Madduri, K.; Hutchinson, C. R. *Biochemistry* **1999**, *38*, 4794–4799.

(41) Thompson, T. B.; Katayama, K.; Watanabe, K.; Hutchinson, C. R.; Rayment, I. *J. Biol. Chem.* **2004**, *279*, 37956–37963.

(42) Kallio, P.; Sultana, A.; Niemi, J.; Mäntsälä, P.; Schneider, G. *J. Mol. Biol.* **2006**, *357*, 210–220.

(43) Kulowski, K.; Wendt-Pienkowski, E.; Han, L.; Yang, K.; Vining, L. C.; Hutchinson, C. R. *J. Am. Chem. Soc.* **1999**, *121*, 1786–1794.

(44) Metsä-Ketelä, M.; Palmu, K.; Kunnari, T.; Ylihonko, K.; Mäntsälä, P. *Antimicrob. Agents Chemother.* **2003**, *47*, 1291–1296.

In conclusion, we have gained new and surprising insights into the biosynthesis of the antibiotic resistomycin, a unique aromatic polyketide with a discoid ring topology. The rare pentacyclic structure results from an unusual S-shaped cyclization that deviates from all other known linear or angular type II PKS pathways. In order to assign the identified cyclases to polyphenol architectures we have performed the first comprehensive sequence-function correlation in a cladogram. While linear and angular pathways generally fit into the scheme of sequential cyclization, cyclases implicated in the discoid biosynthesis clearly deviate. By gene knockout, complementation, and *in vivo* reconstitution, we have identified all components of the *rem* multienzyme complex that are necessary and sufficient for resistomycin formation. Cross-complementation of the noncanonical minimal *rem* PKS (RemABC) and the first ring cyclase (RemI) with corresponding enzymes from the linear tetracenomycin pathway suggested that RemI and TcmN' are functionally equivalent and that both pathways share early biosynthetic steps. We identified two additional cyclases, RemL and RemF, that are required for the controlled cyclization of the reactive decaketide to give rise to the unparalleled naphthanthrene system. In contrast to various other type II PKS pathways, the *rem* cyclases cannot be attributed to individual, stepwise cyclization events. These results provide strong support for a model that includes the multienzyme complex forming a cage in which the polyketide is shaped. Thus, in the *rem* pathway, all components need to work in a highly concerted action in order to yield the polyphenol with the distinct ring topology. Future *in vitro* studies and structural investigations will shed light on the geometry of this multienzyme system orchestrating the cyclization events.

3. Experimental Section

3.1. General. Mass spectra were obtained from an LCQ electrospray MS (Thermo Electron). High-resolution MS spectra were recorded on a MAT 95 XL (Thermo Electron) and a TSQ Quantum Ultra AM (Finnigan). One- and two-dimensional ^1H and ^{13}C NMR spectra were recorded on Bruker AVANCE dpx 300 and drx 500 instruments using the solvent signals as reference. The UV spectra were recorded on a Specord 200 spectrophotometer. IR spectra were obtained on a Sattellite FTIR manufactured by Mattson and a JASCO FT/IR-4100 spectrometer. Thin layer chromatography was performed on silica gel 60 F₂₅₄ plates (layer thickness 0.2 mm, Merck). Analytical HPLC separation was performed on a Nucleosil 100-5, C-18 (3 mm × 125 mm) column, flow rate: 1 mL min⁻¹.

3.2. Phylogenetic Analysis of Cyclases. Sequences of cyclases involved in the resistomycin biosynthetic pathway and of related proteins were mainly retrieved by BLASTp searches (<http://www.ncbi.nlm.nih.gov/>). To isolate the cyclase domain from additional domains InterPro Scan (<http://www.ebi.ac.uk/InterProScan/>) was employed. Amino acid sequences were analyzed with ClustalW⁴⁹ and aligned. The GONNET matrix⁵⁰ was used as the amino acid substitution matrix. The resulting alignment was applied

to the Neighbor-Joining method⁵¹ without manual adjustment. Bootstrapping⁵² was performed to test the reliability of the topology. A phylogenetic tree was drawn by the MEGA 3.1 software.⁵³ The following sequences were used:

3.2.1. Linear. Tetracenomycins. Tetracenomycin; TcmI [AAA67513], TcmJ [AAA67514], TcmN (1–179) [P16559]; Elloramycin, ElmI [AAF73052], ElmJ [AAF73053], ElmNI [CAP12603]. Tetracyclines. Oxytetracycline; OxyI [AAZ78332], OxyK (1–150) [AAZ78334], OxyN [AAZ783379]. *Anthracyclines.* Nogaramycin; SnoaE (1–150)-[CAA12012], SnoaL [AAF01813], SnoaM [AAF01818]. Aclacinomycin; AknE1 (1–150) [BAB72042], AknH [AAF70112], AknW [AAF73459]. Chartreusin; ChaF (1–150) [CAH10156], ChaG [CAH10155], ChaK [CAH10173], ChaJ [CAH10177], ChaU [CAH10171]. Rhodomycin; RdmA [AAA83420]. Daunorubicin; DpsF (1–150) [AAA65203], DpsH [AAD04719], DpsY [AAC38443], DauA (1–150) [AAA87615], DauD [AAB16937]. Steffimycin; StfQ (1–150) [CAJ42327], StfY (1–150) [CAJ42324], StfX [CAJ42323]. *Aureolic acids.* Mithramycin; MtmQ (1–150) [CAA61987], MtmY [CAK50782], MtmX [CAA61988]. Chromomycin; CmmQ (1–150) [CAE17552], CmmY [CAE17518], CmmX [CAE17525]. *BIQs.* Naphthocyclinone; NcnD (1–150) [AAD20270], NcnE [AAD20271]. Granaticin; Gra-Orf4 (1–150) [P16560], GraOrf33 [CAA09660]. Medermycin; Med-Orf3 [BAC79046], Med-Orf19 (1–150) [BAC79027]. Actinorhodin; ActIV [CAC44204], ActVII [Q02055]. Frenolicin; FrnQ (1–150) [AAC18112], FrnR [AAC18113].

3.2.2. Angular. Angucyclines. Sch47554; SchP4 (1–150)-[CAH10113], SchP9 [CAH10118] Gilvocarcin; GilG [AAP69575], GilK (1–150) [AAP69576] Ovidomycin; OvmA (1–150) [CAG14969], OvmC [CAG14964] Simocyclinone; SimA4 [AAK06783], SimA5 (1–150) [AAK06788] Landmycin; LndF [AAU04837], LanF [AAD13535], LanL (1–150) [AAD13540] Jadomycin; JadI [AAD37852], JadII (1–150) [AAB36566]. Urdamycin; UrdF [CAA60568], UrdL (1–150) [AAF00205]. Gaudimycin; PgaF [AAK57524], PgaL (1–150) [AAK57529]. Kinamycin; KinD (1–150) [AAO65350], KinI [AAO65345]. PD116740; Pd2D (1–150) [AAO65366], Pd2I [AAO65361]. Rhodomycin; RdmK (1–150) [AAL24453], *Pentangular polyphenols.* Pradimicin; PdmD [ABM21750], PdmL [ABK58685]. Griseorhodin; GrhE (1–150) [AAM33657], GrhQ [AAM33678], GrhS [AAM33682], GrhT (1–131) [AAM33685], Rubromycin; RubD [AAG03066], RubE [AAG03065], RubF (1–131) [AAG03070] Fredericamycin; FdmD [AAQ08914], FdmE [AAQ08915], FdmI [AAQ08919]. Lysolipin; llpCI [CAM34342], llpCII [CAM34346], llpCIII [CAM34347]. Pradimicin; PdmK [ABM21757]. Benastatin; BenD, BenE, BenH (1–150). Spore pigments. WhiE-OrfII [P23157], WhiE-OrfVI [CAA39411], WhiE-OrfVII [CAB45610], CurC [CAA44379], CurF [Q02572], CurG [CAA44384], SppD [BAC70552], PKSA-ORF4 [AAG26883], PKSA-ORF5 [AAG26882]

3.2.3. Discoid. Resistomycin; RemF [CAE51171], RemI [CAE51178], RemL [CAE51181].

3.3. Plasmids and General DNA Procedures. DNA isolation, plasmid preparation, restriction digests, gel electrophoresis, and ligation reactions were conducted according to standard methods.^{54,55} pBluescript II SK(–) (Stratagene, Amsterdam, NL), pGEM-T Easy (Promega, Mannheim), and pMOSBlue (Amersham Biosciences, Freiburg) were the routine vectors for subcloning and preparation of DNA templates for sequencing. For expression experiments *E. coli-Streptomyces* shuttle vectors pKJ01,⁷ pSET152,⁵⁶ pWHM4*⁵⁵ and SCP2*⁵⁵ were used. Restriction enzyme-digested DNA frag-

(45) Hautala, A.; Torkkell, S.; Rätty, K.; Kunnari, T.; Kantola, J.; Mäntsälä, P.; Hakala, J.; Ylihonko, K. *J. Antibiot.* **2003**, *56*, 143–153.

(46) Lee, T. S.; Khosla, C.; Tang, Y. *J. Am. Chem. Soc.* **2005**, *127*, 12254–12262.

(47) Petkovic, H.; Thamchaipenet, A.; Zhou, L.-H.; Hranueli, D.; Raspor, P.; Waterman, P. G.; Hunter, I. S. *J. Biol. Chem.* **1999**, *274*, 32829–32834.

(48) Meurer, G.; Gerlitz, M.; Wendt-Pienkowski, E.; Vining, L. C.; Rohr, J.; Hutchinson, C. R. *Chem. Biol.* **1997**, *4*, 433–443.

(49) Thompson, J. D.; Gibson, T. J.; Plewniak, F.; Jeanmougin, F.; Higgins, D. G. *Nucleic Acids Res.* **1997**, *25*, 4876–4882.

(50) Gaston, H.; Gonnet, M.; Cohen, A.; Benner, S. *Science* **1992**, *256*, 1443–1445.

(51) Saitou, N.; Nei, M. *Mol. Biol. Evol.* **1987**, *4*, 406–425.

(52) Felsenstein, J. *Evolution* **1985**, *39*, 783–791.

(53) Kumar, S.; Tamura, K.; Nei, M. *Briefings Bioinf.* **2004**, *5*, 150–163.

(54) Sambrook, J.; Fritsch, E. F.; Maniatis, T. *Molecular Cloning: a Laboratory Manual*, 2nd ed.; Cold Spring Harbor: New York, 1989.

(55) Kieser, T.; Bibb, M. J.; Buttner, M. J.; Chater, K. F.; Hopwood, D. A. *Practical Streptomyces Genetics*; The John Innes Foundation: Norwich, U.K., 2000.

(56) Bierman, M.; Logan, R.; O'Brien, K.; Seno, E. T.; Rao, R. N.; Schonher, B. E. *Gene* **1992**, *116*, 43–49.

ments were recovered from agarose gel by the GFX PCR DNA and Gel Band Purification Kit (Amersham).

3.4. Bacterial Strains and Culture Conditions. *S. lividans* TK23 served as host strain for all heterologous expression experiments. For metabolite production, wild-type and mutant strains were cultivated in MS medium (mannitol soya flour medium) for 5 days at 28 °C with shaking. *S. lividans* ZX1 was cultured on R5 agar and YEME liquid medium⁵⁵ for protoplast transformation and on MS (mannitol soya flour)⁵⁷ for all other experiments. Transformants were selected with apramycin or spectinomycin (Sigma) at 50 $\mu\text{g mL}^{-1}$ in both solid and liquid medium. *E. coli* strains DH5 α and XL1 blue served as hosts for routine subcloning.⁵⁴ *E. coli* strains were grown in LB medium supplemented with ampicillin (100 $\mu\text{g mL}^{-1}$) or apramycin (50 $\mu\text{g mL}^{-1}$) for a selection of plasmids.⁵⁴

3.5. Construction of the $\Delta\text{remABDCI}$, ΔremF , ΔremK , and ΔremL Mutants. The *remABDCI*, *remF*, *remK*, and *remL* null mutants were constructed by the λred PCR targeting method^{58–60} as described previously.⁶¹ To amplify the extended streptomycin and spectinomycin resistance gene (*aadA*) flanked by FRT sites (FLP recognition targets), specific long primers were employed. The PCR products were introduced into *E. coli* BW25113/pIJ790 containing cosmid pKJ05, which includes the entire resistomycin biosynthesis gene cluster, with concomitant substitution of the *rem* genes by the extended antibiotic resistance cassette. Primers used for $\Delta\text{remABDCI}$ mutant: KJrem09 (GCT GGT GAC GGC CCA GAC AGG GAA AAG GCG GTA ACC ATG ATT CCG GGG ATC CGT CGA CC) and KJrem10 (GAG GTG CGG GCG GCC GGA GAC CGG CGG CCC GCC GGG TCA TGT AGG CTG GAG CTG CTT C), yielding pKJ81; primers used for ΔremF (full) mutant: KJrem14 (CCG GAT GAC GGG CCC CGC ACA GCG GAA AGG CAG CCG ATG ATT CCG GGG ATC CGT CGA CC) and KJrem15 (CCT GGC CGG CCT GGG TGT CGA GGT CCT GAG TGG TCG TCA TGT AGG CTG GAG CTG CTT C), yielding pKJ71; primers used for ΔremF (partial) mutant: KJrem42 (CAC GAG ATC TAC GTG CTC GAG GGC TCC ATG GGC CTG GTC ATT CCG GGG ATC CGT CGA CC) and KJrem43 (TGC GTG TAC TCG TAG GGG TCC TCG GAG AGG AAC ACG TTG TGT AGG CTG GAG CTG CTT C), yielding pKJ123; primers used for ΔremK mutant: KJrem18 (CTG ATT CCC CTC ACC GTC GCC GGG ATC GTG CCC GGC GTG ATT CCG GGG ATC CGT CGA CC) and KJrem19 (GGC GGC TGA CGG GGA TGC TCA GAT CGA CGA ACA CGG CTA TGT AGG CTG GAG CTG CTT C), yielding pKJ79; primers used for ΔremL mutant: KJrem20 (CCT CCG GCG GCG GCC GGA ACC GAC CGA GGA GTA GCC GTG ATT CCG GGG ATC CGT CGA CC) and KJrem21 (GTC ACC TTG GGG CGG GAC CGG ACT CCT GGA ACC CGG TCA TGT AGG CTG GAG CTG CTT C), yielding pKJ75. The inserted cassette was removed through expression of the FLP-recombinase in *E. coli*. The resulting plasmids were then introduced into *S. lividans* TK23 by protoplast transformation. The metabolic profiles of the transformants were monitored by TLC and HPLC-MS.

3.6. Cloning and Heterologous Expression of *remF* and *remL* for Mutant Complementation. Cyclase genes *remF* and *remL* and their RBS were PCR-amplified using specific primers and pKJ05 as template. For *remF* primer pair KJrem29 (GCT CTA GAC GCT TTC CGT ACG AGG TTT TGA, *XbaI* site underlined) and KJrem46 (CGG ATA TCG GTA GGC GGT CAG GAT GGT GTG GA, *EcoRV* site underlined), and for *remL* primer pair KJrem33 (CGG GAT CCG GAA CCG ACC GAG GAG TAG C,

BamHI site underlined) and KJrem34 (CGG AAT TCG AGG TGG GTG GTG CGG GCG TCG TA, *EcoRI* site underlined) were used. The amplicons were cloned into pGem-T Easy and pBluescript II SK+, respectively, and sequenced. The subclones were then excised and ligated into the *XbaI/EcoRV* (*remF*) or *BamHI/EcoRI* (*remL*) sites downstream of the *ermE* promoter of pKJ55, yielding expression vectors pKJ124 and pKJ105, respectively.

3.7. Cross-Complementation of the $\Delta\text{remABDCI}$ Mutant with *tcm* PKS Genes. For the complementation of the $\Delta\text{remABDCI}$ mutant with the corresponding *tcm* gene cassette the *tsr* resistance marker of pKJ81 needed to be exchanged for *aac(3)IV* in order to yield compatible vectors. This was achieved by PCR targeted recombination in *E. coli* using plasmid pKJ81 and primers KJ27-*tsr* (ATG CGG GGA TCG ACC GCG CGG GTC CCG GAC GGG GAA GAG ATT CCG GGG ATC CGT CGA CC) and KJ35-*tsr* (AGG TCG AGG AAC CGA GCG TCC GAG GAA CAG AGG CGC TTA TGT AGG CTG GAG CTG CTT C) using pIJ773 as template. The resulting plasmid, pKJ87, was not subjected to FLP-mediated recombination but was directly introduced together with pWHM732 (*tcmJKLMN*, *tsrR*) into *S. lividans* TK23 by protoplast transformation.

3.8. Construction of a *remABDCI* Gene Cassette for Heterologous Expression and Pathway Dissection. A 6.5 kb genomic fragment carrying *remABDCIJKL* was obtained by *BsmI* restriction of plasmid pKJ97 and gel-electrophoretic separation, blunted by the Klenow method and cloned into the *HincII* site of pBluescript II SK+, yielding pKJ107. The correct direction of the insert was verified by *XhoI* digestion. A 4.5 kb *remABDCI* fragment was obtained by *XhoI/EcoRV* restriction of pKJ107. The *XhoI* site was blunted (Klenow) prior to ligation into the *EcoRV* site of expression vector pKJ55,¹⁸ yielding plasmid pKJ108. The correct direction of the ligated insert was verified by *HindIII/XbaI* restriction analysis.

3.9. In Vivo Reconstitution of Resistomycin Biosynthesis. Several plasmids compatible with pKJ108 (*remABDCI*) were constructed for successive restoration of the *rem* pathway. Plasmid pKJ104 is a pWHM4* derivative for expression of *remL* that was obtained from cloning the *BamHI/EcoRI* fragment of pKJ100 downstream of the *ermE* promoter of pWHM4*. For expression plasmids pKJ133 and pKJ134 *remG*, *remFG*, and *remL* were PCR-amplified, subcloned into pMOSBlue, and sequenced. Primer pairs for *remG*: KJrem45 (CGG ATA TCG GTG TCC GTC ATT GTGGCG TCC TA, *EcoRV* site underlined) and KJrem47 (GCT CTA GAG GAC CCC TAC GAG TAC ACG CAG AT, *XbaI* site underlined), resulting pMOSBlue derivative: pKJ127; primer pair for *remFG*: KJrem29 (GCT CTA GAC GCT TTC CGT ACG AGG TTT TGA, *XbaI* site underlined) and KJrem45 (CGG ATA TCG GTG TCC GTC ATT GTGGCG TCC TA, *EcoRV* site underlined), resulting pMOSBlue derivative: pKJ126; primer pair for *remL*: KJrem34 (CGG AAT TCG AGG TGG GTG GTG CGG GCG TCG TA, *EcoRI* site underlined) and KJrem44 (CGG ATA TCC GGA ACC GAC CGA GGA GTA GC, *EcoRV* site underlined), resulting pMOSBlue derivative: pKJ125. Then, a 1 kb *EcoRI/EcoRV* fragment containing the *remL* gene was cloned into the corresponding sites in pKJ129 and pKJ130, yielding the gene cassettes *remFGL* (in pKJ131) and *remGL* (in pKJ132), respectively. Transfer of the 2.8 kb (pKJ131) and 2.2 kb (pKJ132) *HindIII/EcoRI* fragments into the SCP2* derivative yielded expression plasmids pKJ133 and pKJ134, respectively. Plasmids pKJ104, pKJ133, and pKJ134 were either subsequently or simultaneously introduced together with pKJ108 into *S. lividans* TK23 by protoplast transformation.

3.10. Isolation and Structure Elucidation of Polyketide Shunt Products. Purification of SEK15 and RM80b. *S. lividans* TK23/pKJ75 was grown on four R5 agar plates at 28 °C for 7 days. The agar was chopped and extracted with ethyl acetate. The extract was dried over Na_2SO_4 and concentrated under reduced pressure. A methanolic solution of the residue was subjected to RP-HPLC (Eurosphere 100-C18, 20 mm \times 250 mm; 25–83% MeCN containing 0.1% TFA; flow rate 10 mL min^{-1} , with UV-detection

(57) Li, A.; Piel, J. *Chem. Biol.* **2002**, *9*, 1017–1026.

(58) Datsenko, K. A.; Wanner, B. L. *Proc. Natl. Acad. Sci. U.S.A.* **2000**, *97*, 6640–6645.

(59) Gust, B.; Challis, G. L.; Fowler, K.; Kieser, T.; Chater, K. F. *Proc. Natl. Acad. Sci. U.S.A.* **2003**, *100*, 1541–1546.

(60) Murphy, K. C.; Campellone, K. G.; Poteete, A. R. *Gene* **2000**, *246*, 321–330.

(61) Xu, Z.; Jakobi, K.; Welzel, K.; Hertweck, C. *Chem. Biol.* **2005**, *12*, 579–588.

at 268 nm) to yield SEK15 (0.2 mg) and RM80b (3.8 mg). Note: Significantly more SEK15 was obtained from a liquid Boe6 culture.

3.10.1. SEK15.³³ HR-ESI-MS, [M + Na]⁺ 407.07420 (calcd for C₂₀H₁₆O₈Na: 407.0737). ¹H NMR (300 MHz, DMSO-*d*₆ at 303 K): δ 12.05 (s, 1H, 1-OH), 11.51 (brs, 1H, aromatic OH), 10.19 (s, 1H, aromatic OH), 10.13 (s, 1H, aromatic OH), 9.81 (s, 1H, aromatic OH), 6.24 (d 2.0, 1H, H8), 6.18 (d 2.0, 1H, H10), 6.11 (d 2.0, 1H, H18), 6.07 (d 2.0, 1H, H16), 5.68 (d 2.0, 1H, H4), 5.15 (d 2.0, 1H, H2), 3.51 (s, 2H, H6), 1.85 (s, 3H, H20). ¹³C NMR (75.5 MHz, DMSO-*d*₆ at 303 K): δ 200.1 (C13), 170.1 (C3), 164.0 (C1), 163.5 (C15), 162.9 (C5), 162.0 (C17), 159.7 (C9), 157.3 (C11), 141.7 (C19), 135.2 (C7), 121.0 (C12), 117.2 (C14), 110.2 (C18), 109.1 (C8), 101.5 (C4), 100.8 (C10), 100.5 (C16), 88.4 (C2), 36.6 (C6), 20.9 (C20).

3.10.2. RM80b.²⁴ HR-ESI-MS, [M + H]⁺ 367.0812 (calcd for C₂₀H₁₅O₇: 367.0812). ¹H NMR (300 MHz, DMSO-*d*₆ at 303 K): δ 11.30 (s, 1H, 1-OH), 10.26 (s, 1H, 13-OH), 10.14 (s, 1H, 11-OH), 7.36 (s, 1H, H8), 6.66 (d 2.2 Hz, 1H, H10), 6.63 (d 2.2 Hz, 1H, H12), 6.18 (s, 1H, H18), 5.43 (d 2.1, 1H, H4), 5.14 (d 2.1, 1H, H2), 4.38 (s, 2H, H6), 2.38 (s, 3H, H20). ¹³C NMR (75.5 MHz, DMSO-*d*₆ at 303 K): δ 177.5 (C17), 170.4 (C3), 166.7 (C5), 163.8 (C19), 159.5 (C11), 156.9 (C15), 138.3 (C9), 130.3 (C7), 126.8 (C8), 115.0 (C16), 111.8 (C18), 107.6 (C14), 103.6 (C12), 101.7 (C10), 98.8 (C4), 87.9 (C2), 19.3 (C20).

3.11. Isolation and Structure Elucidation of Tetracenomyacin R1 (TcmR1). *S. lividans* TK23/pKJ123 was grown on eight R5 agar plates at 28 °C for 7 days. The agar was chopped and extracted with ethyl acetate (800 mL × 3). The extract was dried over Na₂SO₄, concentrated under reduced pressure, and dissolved in MeOH. Purification was achieved by open column chromatography on Sephadex LH20 (25 mm × 460 mm, methanol) followed by RP-HPLC (Eurosphere 100-C18, 20 mm × 250 mm; 50–83% MeCN containing 0.1% TFA; flowrate 10 mL min⁻¹, with UV detection at 280 nm) to yield **TcmR1** (1.5 mg) and tetracenomyacin D3 (2.0 mg).

3.11.1. TcmR1. Dark purple amorphous solid; UV/vis (MeOH) λ_{max} (ε), 210 (26 500), 260 (sh, 26 300), 290 (37 300), 345 (sh, 10 800), 485 (12 100), 509 (13 100); IR (ATR, solid): 1658, 1615, 1573, 1434, 1347, 1315, 1175, 1141, 1123, 1043, 996 cm⁻¹; HR-ESI-MS, *m/z* 379.0466 [M – H]⁻ (calcd for C₂₀H₁₁O₈: 379.0448). NMR data see Table 2.

3.12. Methylation of TcmR1. **TcmR1** (4.0 mg) was dissolved in methanol/benzene (0.8 mL, *v/v* = 1:1) and treated with trimethylsilyldiazomethane (0.5 equiv). The mixture was stirred at room temperature for 3 h, and then acetic acid (10 μL) was added. The crude product was purified by reversed-phase HPLC (Eurosphere 100-C18, 20 mm × 250 mm; 50–83% MeCN containing

Table 2. ¹H and ¹³C NMR Data for Tetracenomyacin R1 and Tetracenomyacin R1 Methyl Ester in DMSO-*d*₆^a

| position | TcmR1 | | TcmR1 methyl ester | |
|----------|-----------------------|------------------------|-----------------------|------------------------|
| | ¹ H (mult) | ¹³ C (mult) | ¹ H (mult) | ¹³ C (mult) |
| 1 | | 167.3 (s) | | 167.4 (s) |
| 2 | | 122.6 (s) | | 122.8 (s) |
| 3 | | 168.1 (s) | | 167.2 (s) |
| 4 | 7.64 (s) | 112.2 (d) | 7.63 (s) | 112.1 (d) |
| 5 | | 137.0 (s) | | 137.5 (s) |
| 6 | | 181.4 (s) | | 181.3 (s) |
| 7 | | 127.8 (s) | | 127.7 (s) |
| 8 | 7.87 (s) | 120.2 (d) | 7.80 (s) | 120.2 (d) |
| 9 | | 138.9 (s) | | 138.9 (s) |
| 10 | 6.92 (s) | 106.4 (d) | 6.86 (s) | 106.3 (d) |
| 11 | 10.63 (s, OH) | 162.0 (s) | 10.57 (s, OH) | 162.0 (s) |
| 12 | 6.57 (s) | 104.9 (d) | 6.52 (s) | 104.8 (d) |
| 13 | | 159.7 (s) | | 159.8 (s) |
| 14 | | 109.7 (s) | | 109.7 (s) |
| 15 | | n.d. | | 158.5 (s) |
| 16 | | 106.3 (s) | | 106.3 (s) |
| 17 | | 186.7 (s) | | 186.4 (s) |
| 18 | | 131.4 (s) | | 129.8 (s) |
| 19 | | 140.4 (s) | | 140.7 (s) |
| 20 | 2.73 (s) | 19.9 (q) | 2.76 (s) | 20.0 (s) |
| Me | | | 4.02 (s) | 52.4 (q) |

^a n.d., not detected.

0.1% TFA, at a flow rate of 10 mL min⁻¹ and UV detection at 280 nm). Recovered starting material was treated and purified as described above twice again, yielding 1.5 mg of tetracenomyacin R1 methyl ester. Dark purple amorphous solid; UV/vis (MeOH) λ_{max} (ε), 220 (10 300), 280 (23 190), 310 (11 800), 333 (sh, 7030), 382 (sh, 4500), 487 (sh, 6400), 510 (7340); IR (ATR, solid): 1762, 1666, 1617, 1574, 1451, 1387, 1349, 1317, 1261, 1158, 1094, 1070, 1046, 1006, 941 cm⁻¹; HR-ESI-MS, *m/z* 393.0600 [M – H]⁻ (calcd for C₂₁H₁₃O₈: 393.0610). NMR data see Table 2.

Acknowledgment. This work has been financially supported by the DFG. We are grateful to C. R. Hutchinson for the kind gift of pWHM732. A. Perner and F. A. Gollmick are acknowledged for performing MS and NMR measurements, respectively.

Supporting Information Available: Additional chromatographic profiles, plasmid construction map, and NMR spectra. This information is available free of charge via the Internet at <http://pubs.acs.org>.

JA800251M